Article

Targeted Cross-Section Calculations For Plasma Simulations

Sebastian Mohr [1,*,†], Maria Tudorovskaya [1,†], Martin Hanicinec [1,2,†] and Jonathan Tennyson [2,†]

1   Quantemol Ltd., 320 Angel, 320 City Road, London EC1V 2NZ, UK; tudorovskaya@gmail.com (M.T.); hanicinecm@quantemol.com (M.H.)
2   Department of Physics and Astronomy, University College, Gower St., London WC1E 6BT, UK; j.tennyson@ucl.ac.uk
*   Correspondence: s.mohr@quantemol.com
†   These authors contributed equally to this work.

Abstract: Gathering data on electron collisions in plasmas is a vital part of conducting plasma simulations. However, data on neutral radicals and neutrals formed in the plasma by reactions between different radicals are usually not readily available. While these cross-sections can be calculated numerically, this is a time-consuming process and it is not clear from the outset which additional cross-sections are needed for a given plasma process. Hence, identifying species for which additional cross-sections are needed in advance is highly advantageous. Here, we present a structured approach to do this. In this, a chemistry set using estimated data for unknown electron collisions is run in a global plasma model. The results are used to rank the species with regard to their influence on densities of important species such as electrons or neutrals inducing desired surface processes. For this, an algorithm based on graph theory is used. The species ranking helps to make an informed decision on which cross-sections need to be calculated to improve the chemistry set and which can be neglected to save time. The validity of this approach is demonstrated through an example in an SF_6/O_2 plasma.

Keywords: cross-section calculations; R-matrix; plasma simulation

1. Introduction

Plasma simulations are vital tools in both academic and industrial settings to investigate plasma discharges in order to gain a better understanding of the underlying processes and improve plasma applications. In general, plasma simulations consist of two domains: the physical model, such as fluid or particle-based numerical model; and the chemistry set which describes the chemical reactions taking place in the plasma. For a successful simulation, both the physical model and the chemistry need to be chosen carefully so that they take all important effects into account; on the other hand, the investigator does not want to spend time on, for example, gathering data on chemical reactions which ultimately do not have a significant influence on the results or include those in the chemistry set which potentially increases the calculation time significantly without any benefit. One type of data which are regularly missing for a complete chemistry set are cross-sections for electron collisions with neutral particles which are formed in the plasma; especially in gas mixtures with multiple molecular gases, new species are created by chemical reactions between the fragments of electron collision dissociation. Such cross-sections can be calculated, for example, with the UK R-Matrix codes [1,2]. However, this is a time-consuming process and calculating cross-sections for all possible species formed might not be necessary as their impact on important plasma parameters such as the density of electrons or neutrals participating in desired surface reactions is negligible. Therefore, we present a structured approach to identify species which have a significant influence on the discharge before conducting precise cross-section calculations; this allows the investigator to improve the chemistry set without spending time on unnecessary calculations. The paper is structured

as follows: First we present the different steps in this approach. It requires running a global plasma model, so a short overview of the model used is given. Then the method, based on the directed relation graph theory [3–6], of identifying key species for which cross-sectional data are missing is presented. This is followed by an overview of the actual cross-section calculations. After the general discussion, an example of using this method for an SF_6/O_2 plasma [7–17] is given, showing the impact of adding new cross-sectional data to a chemistry set using estimated data for electron collisions. Finally, conclusions are drawn.

2. Materials and Methods

In this work, we present a methodical approach to identify species with unknown cross-sections in a plasma chemistry set for which precise cross-section calculations improve the accuracy of the plasma simulation significantly. On the other hand, this also prevents one from performing time-consuming cross-section calculations which ultimately will not have a significant influence. This method consists of three steps:

- Running a plasma simulation;
- Identifying species significantly influencing the densities of specified target species;
- Calculating missing cross-sections.

2.1. Plasma Simulation

In the first step, a plasma simulation is conducted to produce densities and, specifically, production and consumption rates in both the gas phase and via plasma-surface interactions. In general, any kind of plasma simulation from which these rates can be extracted can be used; to keep the calculation time short, a global plasma model is the recommended choice, however. In this work, we use the Quantemol GlobalModel which is available online in Quantemol DataBase (QDB) [18], a plasma chemistry database. Detailed documentation can also be found in QDB, see https://quantemoldb.com as of 20 October 2021. In short, this global model solves the reactor-averaged continuity equations for heavy particles and the electron energy balance equation. The electron density is obtained via charge neutrality. The input parameters are power, pressure, neutral gas temperature, flows, and geometrical factors to determine the power density and diffusive losses. Rates for chemical reactions, for both electrons and ions, are characterised by parameterized rate coefficients; currently the modified Arrhenius form is supported. The values of the parameters can be obtained from Maxwellian electron energy distribution functions (EEDF) or ones obtained from a Boltzmann solver by fitting them to a set of electron temperature–rate coefficient pairs. In this work, Maxwellian EEDFs were used to keep the calculation time short. The result of the global model comprises the densities of all used species and the electron temperature. From these, the rates for both gas phase and plasma–surface interactions can easily be obtained in combination with the reaction set and the geometrical factors. In order to use the model to identify important species with missing cross-sections, electron collisions for these species need to be included. In the absence of precise data, this means that estimated rate coefficients, for example in analogy to the same processes for similar species, must be used. This way, the influence of a specific species can at least be estimated, if not precisely predicted.

2.2. Identifying Key Species

An algorithmic method is used to identify which species have a significant influence on the modelled densities of the set of user-specified species, referred to as species of interest. The set of species of interest is one of the inputs to the method, and needs to be identified by the researcher. The species of interest will generally be tailored to a specific modelling application. As an example, some major etchant species might be appropriately identified as species of interest for a specific etching process model, as well as electrons (as the electron density is a fundamental plasma parameter). The method is loosely based on the directed relation graph (DRG) theory of Lu and Law [3–5], originally developed

for the combustion modelling community, but adapted for a plasma environment and expanded to also include the effects of plasma–surface interactions. Only a brief overview of the algorithm is given here, while the reader is referred to the full description of the fast graph–theoretical species ranking method given in [6].

To identify which species significantly influence the densities of some of the specified species of interest, a directed graph is instantiated with all the species present in the modelled system represented by the graph nodes. The directed edges in the graph are weighted by the direct interaction coefficients, which are generally functions of the reaction rates R_j of the volumetric and surface reactions in the chemistry set, and represent a measure of asymmetric coupling between two species (or the edge nodes) that are directly related through some of the reactions. Coupling between two species, however, exists even if they do not share any elementary reactions. The *indirect asymmetric coupling coefficients* W_{AB} between species A and B are therefore defined, reflecting the global (often indirect) effect of the presence of species A (or rather all of its reactions) on the modeled density of the species B. The indirect coupling coefficients are computed by a methodology based on the well-established Dijkstra's search for the "shortest path" in the chemistry graph [19].

Each species X_i is then given a ranking score C, such as

$$C_i = \max_k W_{X_i X_k},\tag{1}$$

where the index k runs over all the species of interest specified by the user, while the index i runs over all the remaining species. The input to the method (next to the set of species of interest) are the reaction rates of all the volumetric and surface reactions in the chemistry set (obtained from the plasma simulation, as described in Section 2.1) The output is a listing of all the species (except the species of interest), ranked with regard to how much they influence the densities of the species of interest. This allows one to make an informed decision on what additional rigorous cross-section calculations are required. It should be noted that there is no strict criterion on which ranking score threshold distinguishes significant species, so this still lies within one's discretion. For example, one might first aim to calculate cross-sections for reactions without precise data involving the higher-ranked species, and if that proves not to change the results for the species of interest significantly, one might neglect the lower-ranked species.

2.3. Cross-Section Calculations

In this work, ionization and dissociation cross-sections for SOF_4 are calculated with the QEC (Quantemol-Electron Collisions) software developed by Quantemol Ltd for calculating electron collision properties [2]. The calculations are based on the ab initio R-Matrix theory [20], specifically, it employs the UKRmol+ code suite [1]. In order to ensure good convergence, the cc-pVDZ basis set and configuration interaction level of theory was employed for the calculations allowing for excited electron configurations. There were 52 electrons frozen in 26 orbitals, while the active space was 4 fully occupied and 4 virtual orbitals.

Ionization cross-sections are calculated using the semi-empirical Binary-Encounter-Bethe (BEB) method [21]. The implementation of BEB within QEC uses Hartree–Fock wave functions and Koopman's theorem to provide thresholds to ionization [22] which are obtained from the quantum chemistry code MOLPRO [23].

The total dissociation cross-sections are obtained by adding up the excitation cross-sections to dissociative states of the target molecule. The dissociation limit is calculated by building a potential energy curve. Stretching the S-F bond(s) and the S-O bond and calculating the total energies at these stretched geometries is carried out in order to determine the most likely ionisation channel. We find that S-F bond breaking is more likely to occur. In this approximation, the state is considered dissociative if the excitation energy exceeds the dissociation energy. According to [24], the bond strength is 4.2 eV while the excited state is found at 8.5 eV above the ground state. Therefore, we consider all excited states

dissociative. Moreover, the excitation energy is more than twice the bond breaking energy, and we assume that 2 S-F bonds will be broken in the dissociation process.

3. Example SF$_6$/O$_2$ Plasma

SF$_6$/O$_2$ discharges are commonly used, for example, for etching silicon [7–17]. The main chemical etchant is atomic F [10,11,14,16,17]. The addition of oxygen can serve two purposes; they induce reactions of the form

$$\text{SF}_x + \text{O} \rightarrow \text{SOF}_{x-1} + \text{F} \tag{2}$$

which increase the density of atomic F [7,9,16]. On the other hand, oxygen atoms can form a protective layer on the side wall of an etched trench, prohibiting isotropic chemical etching by F [8,11–15,17]. Cross-section sets for SF$_6$ and O$_2$ separately are quite easily obtained. However, no such data exist in ready-to-use form for the SOF$_x$ species generated by reaction (2). It is, however, conceivable that under specific process conditions, the ionization and dissociation of these species can significantly contribute to the respective production processes as well as the collisional electron energy losses. Hence, we present an example of how to use the discussed method to identify significant missing cross-sections and their calculation.

For the first step, the initial plasma simulation, we constructed an SF$_6$/O$_2$ set the following way:
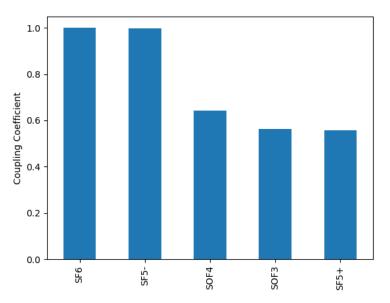
- Electron collision processes for O$_2$ and O species were taken from [25–27];
- Electron collision processes for SF$_x$ were taken from [28–30];
- Electron collision processes for F were taken from [31];
- Neutral–Neutral reactions, specifically the creation of SOF$_x$ species, were taken from [7];
- Ion–Ion recombination and charge exchange, both symmetric and asymmetric, were included for all possible combinations with generic rate coefficients;
- Electron collision ionization and dissociation for SOF$_x$ were included with estimated rate coefficients in analogy to SF$_x$, e.g., SF$_5$ rate coefficients were used for SOF$_4$. We assumed that the neutral dissociation process splits one F and the ionization produces the SOF$_x^+$ ion. One exception is SOF$_4$ which produces SOF$_3^+$ + F on ionization.

For similar reaction sets used in plasma simulations see, for example, [15,16]

The global model was run using this set with the following process parameters:

- Power: 500 W;
- Pressure: 10 Pa;
- Radius: 10 cm;
- Height: 10 cm;
- Total flow: 100 sccm;
- Relative oxygen flow: 10–90%.

It should be noted that these process parameters are not intended to reproduce a specific experiment/process but were chosen to demonstrate the effect of using our proposed method.

The species ranking algorithm was employed with F and electrons as species of interest. Figure 1 shows the 5 highest ranking species for a relative oxygen flow of 50%. Out of the SOF$_x$ species SOF$_4$ and SOF$_3$ are among them, with SOF$_4$ ranking higher. Thus, ionization and dissociation cross-sections for SOF$_4$ were calculated.

Figure 1. Species ranking with regard to the productions of electrons and F for a relative oxygen flow of 50%. Cross-sections for all SOF_x species are estimated.
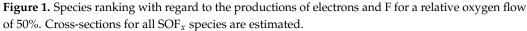
Figure 2 shows the calculated ionization cross-section and resulting rate coefficient in comparison with the estimated one; Figure 3 shows the same for the dissociation. We observe some major differences:

- The calculated ionization cross-section is significantly larger than the estimated ones, by about a factor of 4 throughout the entire energy range up to a 1000 eV. However, the threshold energy is also larger, 15.19 eV compared to 11.8 eV for the estimated cross-sections. As a result, the ionization rate coefficient for the calculated cross-section is smaller for low electron temperatures and larger for high electron temperatures. The rate coefficients differ by about a factor of 2 at most.
- While the calculated dissociation cross-section shows significantly smaller values over a large range of energies, it also has a lower threshold energy; concerning the rate coefficients, the larger values of the estimated cross-section has a larger influence than the higher threshold energy. Hence, the estimated rate coefficient is significantly larger than the precisely calculated one over the majority of the investigated electron temperature range.
- The analysis of the neutral dissociation also showed that a breakup into $SOF_2 + 2F$ is more likely than into $SOF_3 + F$ (see the explanation above). Hence, this dissociation reaction was also changed with regard to the reaction products.
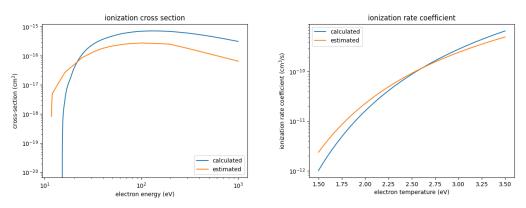

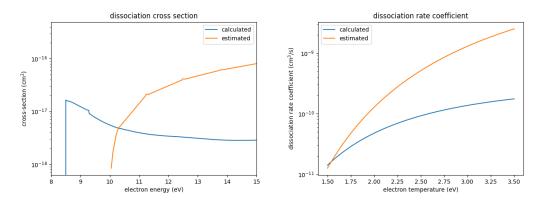**Figure 2.** Calculated and estimated ionization cross-section and rate coefficient for SOF_4.

Figure 3. Calculated and estimated dissociation cross-section and rate coefficient for SOF_4.

To illustrate the effect of using calculated cross-sections instead of estimated ones, Figure 4 shows the density for F and electrons for a varied oxygen flow under otherwise the same process conditions. The calculated, precise cross-sections yield consistently higher densities of both F and electrons; only for very small oxygen flows <20% no significant difference is observed.
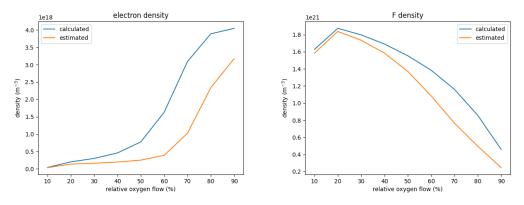

Figure 4. Electron and F density for a variation of the relative oxygen flow. The graphs compare the respective densities between the chemistry set with precisely calculated and the set with estimated cross-sections for the dissociation and ionization of SOF_4.

The higher density of F for the set with the calculated cross-sections can be explained by the significantly higher electron density which increases the production of F from SOF_4 despite the smaller rate coefficient. The higher electron density in turn is a result of differences in the energy necessary to create one electron-ion pair ϵ. This is defined as

$$\epsilon = \epsilon_{ion} + \sum_i \frac{\epsilon_i k_i}{k_{ion}} \tag{3}$$

with the ionization potential ϵ_{ion}, the characteristic energy loss per collision ϵ_i and the rate coefficients k_{ion} for ionization and k_i for other electron collisions. The sum is taken over all other collision types. This parameter determines the plasma density achieved in a given gas mixture; the lower ϵ, the higher the plasma density. Figure 5 shows this energy for SOF_4 using the estimated and calculated rate coefficients. As can be seen, ϵ is about an order of magnitude smaller for the calculated rate coefficients, mostly as a result of the much smaller rate coefficient for dissociation. For relative oxygen flows above 20%, SOF_4 is one of the most abundant neutrals, only topped by either F or O. Figure 6 shows the ϵ for SOF_4, F, and O weighted by their relative densities for each simulated case. As can be seen, when using the estimated cross-sections, electron collisions with SOF_4 significantly contribute to the collisional energy losses and can even be the major contributors. When using the precisely calculated ones, however, its weighted ϵ is at least one order of magnitude smaller

than either the one for F or O both of which do not differ significantly between the different sets. This leads to the significantly increased electron density for the set using calculated cross-sections.
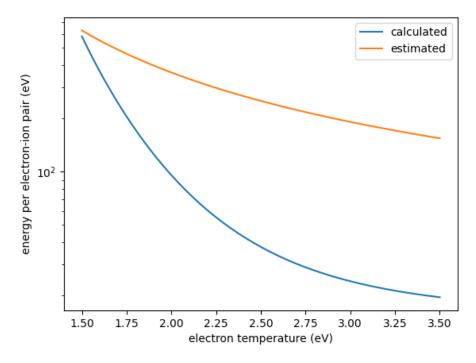

Figure 5. Energy per electron–ion pair for SOF_4 as a function of electron temperature derived from calculated and estimated cross-sections.
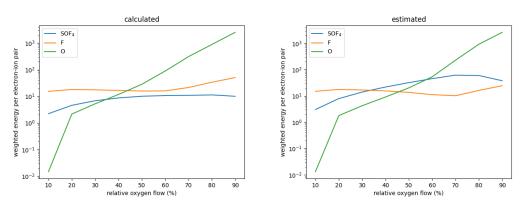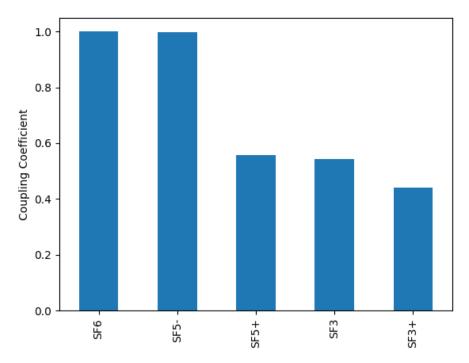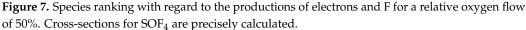

Figure 6. Electron energy per electron–ion pair weighted by their respective relative densities for SOF_4, F, and O as a function of the relative oxygen flows.

Furthermore, if we repeat the ranking on the simulation using the calculated cross-sections, we see in Figure 7 that SOF_3 is now missing from the top-ranked species due to the missing dissociation channel from SOF_4. Other SOF_x also do not appear, so it is unlikely that calculation of cross-sections for these would improve the simulation significantly. Therefore, by doing the analysis via the species ranking we could

- improve the accuracy of our plasma simulation by calculating precise cross-sections which were formerly missing and had to be estimated;
- save time by ruling out species for which precise cross-section calculations will unlikely improve the simulation significantly.

Figure 7. Species ranking with regard to the productions of electrons and F for a relative oxygen flow of 50%. Cross-sections for SOF_4 are precisely calculated.

4. Conclusions

We have presented a method to identify important missing cross-sections in a chemistry set and how adding them to a chemistry set affects the results of plasma simulations. The method consists of three steps:

- Run a plasma simulation such as a global model with a chemistry set containing estimates for missing cross-sections.
- Use the results of the plasma simulation in a species ranking algorithm. This identifies the species with missing cross-sections who potentially influence the densities of target species such as major etchants.
- Calculate precise cross-sections for high-ranking species and substitute these for the estimated ones.

This method gives a fast option to identify for which species precise cross-sections are needed and for which more precise data are not necessary to significantly improve the results of the simulation, preventing wasted time on unnecessary calculations.

This method was demonstrated for an SF_6/O_2 plasma. For a specific set of process conditions, SOF_4 and SOF_3 were identified as potential targets for precise cross-section calculations. As higher-ranking species, first only cross-sections for SOF_4 were calculated. Adding them to the existing set showed major differences in both the density of F and electrons. Furthermore, SOF_3 was not among the highest-ranking species anymore, so the calculation of cross-sections for this species could be skipped. Hence, the suitability of the proposed method to quickly improve plasma simulations via targeted cross-sections calculations was demonstrated.

Author Contributions: S.M. carried out the plasma simulations and analysis of its results. M.T. calculated the cross-sections for SOF_4. M.H. wrote the global model and the ranking algorithm. J.T. advised on the cross-section calculations and ranking algorithm. All authors have read and agreed to the published version of the manuscript.

Data Availability Statement: Reactions data used in this project is available from the QDB database.

Conflicts of Interest: All authors declare an involvement with Quantemol Ltd. who retail both the QEC expert system and the QDB database.

References

1. Mašín, Z.; Benda, J.; Gorfinkiel, J.D.; Harvey, A.G.; Tennyson, J. UKRmol+: A suite for modelling of electronic processes in molecules interacting with electrons, positrons and photons using the R-matrix method. *Comput. Phys. Commun.* **2020**, *249*, 107092. [CrossRef]
2. Cooper, B.; Tudorovskaya, M.; Mohr, S.; O'Hare, A.; Hanicinec, M.; Dzarasova, A.; Gorfinkiel, J.; Benda, J.; Mašín, Z.; Al-Refaie, A.; et al. Quantemol Electron Collision: An expert system for performing UKRmol+ electron molecule collision calculations. *Atoms* **2019**, *7*, 97. [CrossRef]
3. Lu, T.; Law, C.K. A directed relation graph method for mechanism reduction. *Proc. Combust. Inst.* **2005**, *30*, 1333–1341. [CrossRef]
4. Lu, T.; Law, C.K. Linear time reduction of large kinetic mechanisms with directed relation graph: n-Heptane and iso-octane. *Combust. Flame* **2006**, *144*, 24–36. [CrossRef]
5. Lu, T.; Law, C.K. On the applicability of directed relation graphs to the reduction of reaction mechanisms. *Combust. Flame* **2006**, *146*, 472–483. [CrossRef]
6. Hanicinec, M.; Mohr, S.; Tennyson, J. Fast species ranking for iterative species-oriented skeletal reduction of chemistry sets. *Plasma Sources Sci. Technol.* **2021**, *29*, 125024. [CrossRef]
7. Ryan, K.R.; Plumb, I.C. A model for the etching of silicon in SF_6/O_2 plasmas. *Plasma Chem. Plasma Process.* **1990**, *10*, 207–229. [CrossRef]
8. Bartha, J.W.; Greschner, J.; Puech, M.; Maquin, P. Low temperature etching of Si in high density plasma using SF_6/O_2. *Microelectron. Eng.* **1995**, *27*, 453–456. [CrossRef]
9. Pateau, A.; Rhallabi, A.; Fernandez, M.C.; Boufnichel, M.; Roqueta, F. Modeling of inductively coupled plasma $SF_6/O_2/Ar$ plasma discharge: Effect of O_2 on the plasma kinetic properties. *J. Vac. Sci. Technol. A* **2014**, *32*, 021303. [CrossRef]
10. Maruyama, T.; Narukage, T.; Onuki, R.; Fujiwara, N. High-aspect-ratio deep Si etching in SF_6/O_2 plasma. I. Characteristics of radical reactions with high-aspect-ratio patterns. *J. Vac. Sci. Technol. B* **2010**, *28*, 854–861. [CrossRef]
11. Gomez, S.; Jun Belen, R.; Kiehlbauch, M.; Aydil, E.S. Etching of high aspect ratio structures in Si using SF_6/O_2 plasma. *J. Vac. Sci. Technol. A* **2004**, *22*, 606–615. [CrossRef]
12. Aachboun, S.; Ranson, P. Deep anisotropic etching of silicon. *J. Vac. Sci. Technol. A* **1999**, *17*, 2270–2273. [CrossRef]
13. Boufnichel, M.; Aachboun, S.; Grangeon, F.; Lefaucheux, P.; Ranson, P. Profile control of high aspect ratio trenches of silicon. I. Effect of process parameters on local bowing. *J. Vac. Sci. Technol. B Microelectron. Nanometer Struct. Process. Meas. Phenom.* **2002**, *20*, 1508–1513. [CrossRef]
14. Blauw, M.A.; van der Drift, E.; Marcos, G.; Rhallabi, A. Modeling of fluorine-based high-density plasma etching of anisotropic silicon trenches with oxygen sidewall passivation. *J. Appl. Phys.* **2003**, *94*, 6311–6318. [CrossRef]
15. Anderson, H.M.; Merson, J.A.; Light, R.W. A Kinetic Model for Plasma Etching Silicon in a SF_6/O_2 RF Discharge. *IEEE Trans. Plasma Sci.* **1986**, *14*, 156–164. [CrossRef]
16. Rauf, S.; Dauksher, W.J.; Clemens, S.B.; Smith, K.H. Model for a multiple-step deep Si etch process. *J. Vac. Sci. Technol. A* **2002**, *20*, 1177–1190. [CrossRef]
17. Marcos, G.; Rhallabi, A.; Ranson, P. Topographic and kinetic effects of the SF_6/O_2 rate during a cryogenic etching process of silicon. *J. Vac. Sci. Technol. B Microelectron. Nanometer Struct. Process. Meas. Phenom.* **2004**, *22*, 1912–1922. [CrossRef]
18. Tennyson, J.; Rahimi, S.; Hill, C.; Tse, L.; Vibhakar, A.; Akello-Egwel, D.; Brown, D.B.; Dzarasova, A.; Hamilton, J.R.; Jaksch, D.; et al. QDB: A new database of plasma chemistries and reactions. *Plasma Sources Sci. Technol.* **2017**, *26*, 055014. [CrossRef]
19. Dijkstra, E.W. A note on two problems in connexion with graphs. *Numer. Math.* **1959**, *1*, 269–271. [CrossRef]
20. Tennyson, J. Electron-molecule collision calculations using the R-matrix method. *Phys. Rep.* **2010**, *491*, 29–76. [CrossRef]
21. Kim, Y.K.; Rudd, M.E. Binary-encounter-dipole model for electron-impact ionization. *Phys. Rev. A* **1994**, *50*, 3945. [CrossRef]
22. Graves, V.; Cooper, B.; Tennyson, J. The efficient calculation of electron impact ionization cross sections with effective core potential. *J. Chem. Phys.* **2021**, *154*, 114104. [CrossRef]
23. Werner, H.J.; Knowles, P.J.; Knizia, G.; Manby, F.R.; Schütz, M. Molpro: A general-purpose quantum chemistry program package. *WIREs Comput. Mol. Sci.* **2012**, *2*, 242–253. [CrossRef]
24. Herron, J.T. Thermochemical Data on Gas Phase Compounds of Sulfur, Fluorine, Oxygen, and Hydrogen Related to Pyrolysis and Oxidation of Sulfur Hexafluoride. *J. Phys. Chem. Ref. Data* **1987**, *16*, 1. [CrossRef]
25. Phelps, A.V. *Tabulations of Collision Cross Sections and Calculated Transport and Reaction Coefficients for Electron Collisions with O_2*; Technical Report; University of Colorado: Boulder, CO, USA, 1985.
26. Krishnakumar, E.; Srivastava, S.K. Cross-sections for electron impact ionization of O_2. *Int. J. Mass Spectrom. Ion Process.* **1992**, *113*, 1–12. [CrossRef]
27. Itikawa, Y.; Ichimura, A. Cross Sections for Collisions of Electrons and Photons with Atomic Oxygen. *J. Phys. Chem. Ref. Data* **1990**, *19*, 637. [CrossRef]
28. Christophorou, L.G.; Olthoff, J.K. Electron Interactions with SF_6. *J. Phys. Chem. Ref. Data* **2000**, *29*, 267–330. [CrossRef]

29. Tarnovsky, V.; Deutsch, H.; Martus, K.E.; Becker, K. Electron impact ionization of the SF_5 and SF_3 free radicals. *J. Chem. Phys.* **1998**, *109*, 6596–6600. [CrossRef]

30. Phelps, A.V.; Van Brunt, R.J. Electron-transport, ionization, attachment, and dissociation coefficients in SF_6 and its mixtures. *J. Appl. Phys.* **1988**, *64*, 4269–4277. [CrossRef]

31. Morgan, W.L. (Kinema Research and Software). Personal Communication.